ELSEVIER
0966-9795(95)00008-9
Intermetallics 3 (1995) 493–503

0966-9795/95/$09.50

NiAl-based polyphase *in situ* composites in the NiAl–Ta–*X* (*X* = Cr, Mo, or V) systems

D. R. Johnson,[a]* B. F. Oliver,[a] R. D. Noebe[b] & J. D. Whittenberger[b]

[a]*Material Science and Engineering Department, University of Tennessee, Knoxville, Tennessee 37996–2200, USA*
[b]*NASA Lewis Research Center, Cleveland, Ohio 44135, USA*

(Received 12 December 1994; accepted 26 January 1995)

Polyphase *in situ* composites were generated by directional solidification of ternary eutectics. This work was performed to discover if a balance of properties could be produced by combining the NiAl–Laves phase and the NiAl–refractory metal phase eutectics. The systems investigated were the Ni–Al–Ta–*X* (*X* = Cr, Mo, or V) alloys. Ternary eutectics were found in each of these systems and the eutectic composition, temperature, and morphology were determined. The ternary eutectic systems examined were the NiAl–NiAlTa–(Mo, Ta), NiAl–(Cr, Al) NiTa–Cr, and the NiAl–NiAlTa–V systems. Each eutectic consists of NiAl, a C14 Laves phase, and a refractory metal phase. Directional solidification was performed by containerless processing techniques in a levitation zone refiner to minimize alloy contamination. Room temperature fracture toughness of these materials was determined by a four-point bend test. Preliminary creep behavior was determined by compression tests at elevated temperatures, 1100–1400 K. Of the ternary eutectics, the one in the NiAl–Ta–Cr system was found to be the most promising. The fracture toughness of the NiAl–(Cr, Al)NiTa–Cr eutectic was intermediate between the values of the NiAl–NiAlTa eutectic and the NiAl–Cr eutectic. The creep strength of this ternary eutectic was similar to or greater than that of the NiAl–Cr eutectic.

Key words: NiAl, *in situ* composites, processing, creep

INTRODUCTION

Ordered intermetallics such as NiAl are considered candidates for high temperature structural applications, provided that the proper combination of room temperature toughness and elevated temperature strength can be developed. However, processing of intermetallics is usually difficult due to their refractory nature. Before mechanical properties can be measured and optimized, processing routes must produce sound bulk material which can be reliably tested. Improvements in all these areas are generally found for multi-phase alloys.

One of the major difficulties in producing composite materials for elevated temperature use is the selection of materials that will be thermodynamically compatible and stable at the targeted application temperature. An advantage of producing multi-phase material from eutectic alloys is that phases are thermodynamically stable at temperatures up to the melting point. Directional solidification of these eutectic alloys may produce *in situ* composites where one or more phases are aligned parallel to the growth direction.

Of particular interest are polyphase *in situ* composites which are defined here as directionally solidified eutectics resulting in three or more phases. The basic idea is to include a metallic phase for improved room temperature toughness with a number of intermetallic phases for good high temperature properties. For example, the NiAl–(Cr, Mo) eutectic has a promising room temperature fracture toughness[1] while the NiAl–NiAlTa eutectic has a very good creep strength.[2] Thus, it may be possible to blend the properties of each system in a directionally solidified three phase eutectic, provided such systems thermodynamically exist.

The disadvantages of working with eutectic alloys are the limited composition ranges where couple growth may take place. In addition, the phase diagrams for many systems of interest are unknown. Hence, the purpose of this investigation was to locate multi-phase eutectic systems for directional solidification and to briefly examine their mechanical properties.

*Presently at: Department of Metal Science and Technology, Kyoto University, Sakyo-ku, Kyoto, 606, Japan.

The strategy used in the alloy design was based upon trying to combine the good room temperature properties of the NiAl–refractory metal eutectics with the good elevated temperature properties of the NiAl–Laves phase eutectics (such as NiAl-NiAlTa). The alloys considered were from the Ni–Al–Ta–X (X = refractory metal) system. Other alloying work in these systems has emphasized the nickel rich alloys.[5–8] In addition to chromium, NiAl undergoes a eutectic reaction with the refractory metals Mo, V, W and Re.[3] However, since the volume fractions of Re and W are very small in the quasi-binary eutectics, these alloys were not examined. In addition, due to the poor oxidation resistance of vanadium, alloys containing vanadium were studied only as a model system. The NiAl–V eutectic is of interest due to its excellent fracture toughness at room temperature, 40 MPa$\sqrt{m}$.[4] Therefore, only the Ni–Al–Ta–X (X = Cr, Mo or V) systems were considered.

EXPERIMENTAL PROCEDURES

As a first approach to locating promising microstructures for *in situ* composites studies, exploratory arc-melts containing high purity Ni, Al, Ta, Cr, Mo and V were made. These ingots were metallographically examined for evidence of eutectic-like microstructures. Alloy compositions were then varied to increase the eutectic volume fraction.

Since the arc-melted ingots had an extremely fine microstructure, a coarsening heat treatment was performed to better characterize the microstructure. Heat treatments were performed in an induction furnace using a helium atmosphere. Specimens were wrapped in tantalum foil and placed in an alumina crucible that was surrounded by a graphite susceptor. Temperature measurements were made with an optical pyrometer assuming black body conditions at the gap between the alumina crucible and the graphite susceptor.

Small induction melts (25 g) were also made from promising alloy compositions to better characterize the solidification microstructure. The induction melts were allowed to cool within the alumina crucible, providing a much slower cooling rate and coarser microstructure than the arc-melted ingots. Lastly, larger ingots were prepared for directional solidification. Precursor ingots were produced by induction melting of a 1 kg charge that was chill cast into a copper mold. After removal of the hot-top, the precursor ingots were nominally 25 mm in diameter and 300 mm in length. Containerless directional solidification was performed with electromagnetically-levitated and constrained liquid zones at 19 mm/h to produce near-equilibrium microstructures. Details of the

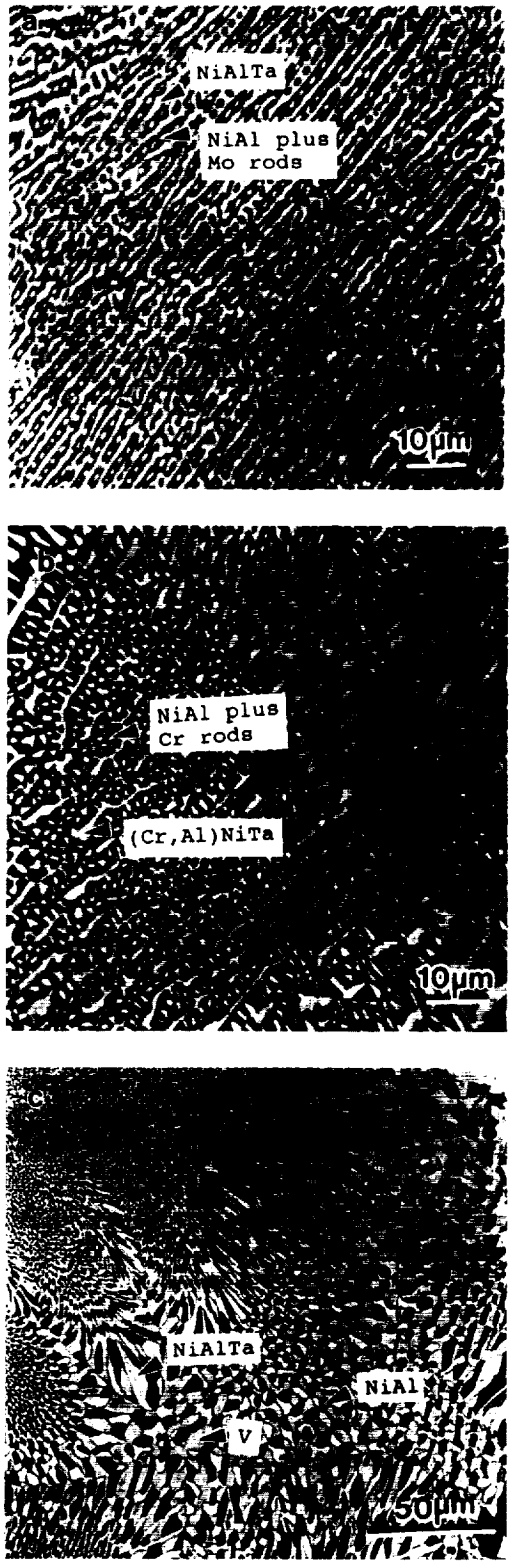

Fig. 1. Light optical photomicrograph of ternary eutectics consisting of NiAl, a Laves phase, and a refractory metal. (a) NiAl–NiAlTa–(Mo, Ta); (b) NiAl–(Cr, Al)NiTa–Cr, and (c) NiAl–NiAlTa–V.

directional solidification procedure and equipment are presented elsewhere.[1,2,9]

The room temperature toughness of the directionally solidified alloys was determined by performing four-point bend tests with an outer/inner loading span of 30 and 15 mm respectively. Bend specimens were electrical discharge machined from the directionally solidified ingots and notched perpendicular to the growth direction using a slow speed diamond impregnated saw. A fatigue crack was not initiated at the notch tip prior to testing. Bend tests were performed on a screw driven test frame using a displacement rate of $1{\cdot}4 \times 10^{-4}$ mm/s.

The elevated temperature strengths of the directionally solidified eutectics were determined by compressions tests between 1100 and 1400 K. Cylindrical compression specimens, 5 mm diameter by 10 mm length, with the compression axis parallel to the growth direction, were electrical discharge machined from selected ingots. Mechanical properties were generated under both constant velocity conditions in a screw driven universal machine and under constant load conditions in lever-arm creep machines at temperatures between 1100 and 1400 K. Constant velocity experiments were used to determine the behavior at fast strain rates ($> 10^{-7}$ s^{-1}) while constant load testing was employed for slower rates. All testing was performed in air as a secondary check for environmental resistance under load.

MICROSTRUCTURES

Ternary eutectic microstructures consisting of NiAl, a Laves phase, and a metal phase were found in all three of the Ni–Al–Ta–X (X = Cr, Mo, V) systems. The eutectic microstructure from the small induction melts for each system is shown in Fig. 1. The approximate eutectic composition, melting point of each eutectic and the volume fraction of each phase are listed in Table 1. Identification of each phase was determined from X-ray diffractometer scans. The Laves phase in all three alloys was found to have the hexagonal C14 crystal structure with lattice parameter values near a = 0·49 and c = 0·80 nm. The melting point of each alloy was determined by differential thermal analysis (DTA). The volume fraction of each phase was

Table 1. Melting point and volume fraction of each phase for ternary eutectics in the NiAl–NiAlTa–refractory metal systems. Values for the volume fraction calculated by the lever rule are enclosed by parantheses

Alloy (at%)	Melting point (K)	Volume Fraction		
		NiAl	Laves	Metal
Ni–42Al–12·5Ta–7Mo	1800	57 (60)	33 (29)	10 (11)
Ni–30·5Al–6Ta–33Cr	1700	40 (53)	25 (17)	35 (30)
Ni–28·5Al–10Ta–33V	1615	24 (26)	32 (29)	44 (45)

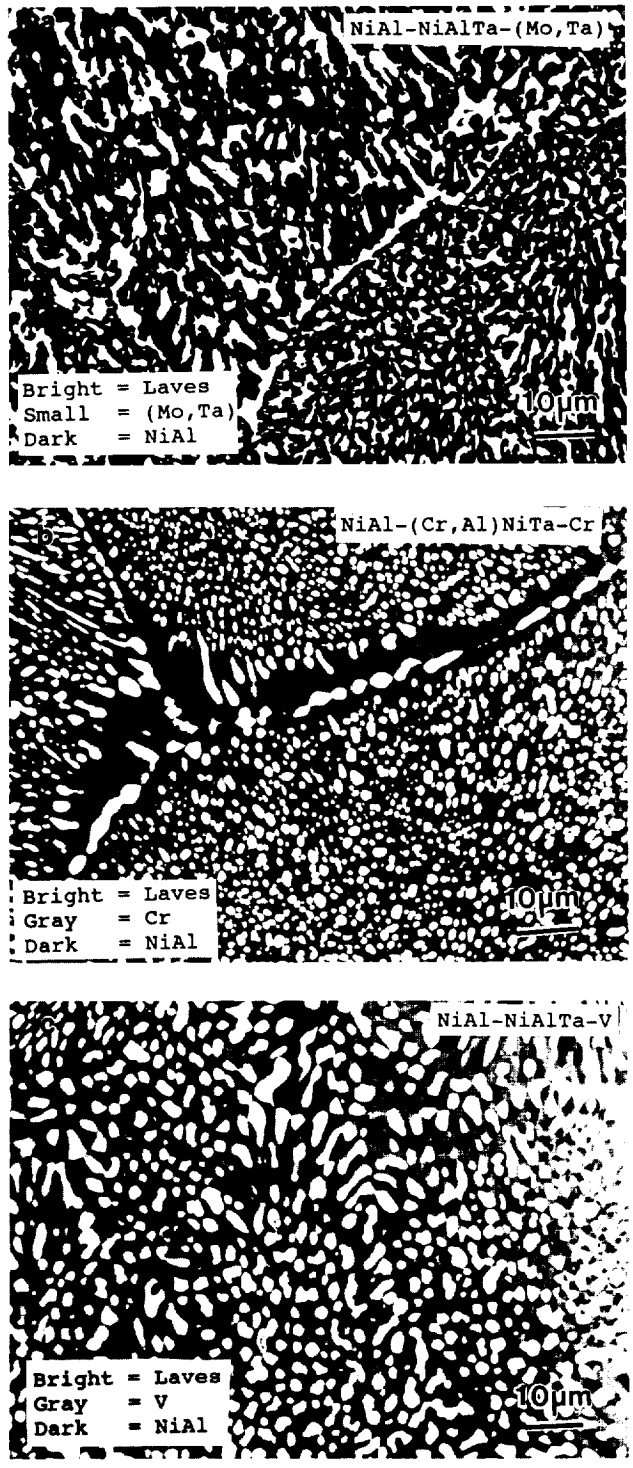

Fig. 2. SEM backscattered electron images of arc-melted after heat treating. (a) NiAl–NiAlTa–(Mo, Ta) at 1673 K for 14·4 ks; (b) NiAl–(Cr, Al)NiTa–Cr at 1673 K for 14·4 ks, and (c) NiAl–NiAlTa–V at 1533 K for 14·4 ks.

measured from SEM backscattered electron photomicrographs of the directionally solidified material.

In addition to the morphology of the composite solidification microstructure, the phase stability at elevated tempratures involves the susceptibility of the microstructure to coarsensing and the phase equilibria for temperatures below the eutectic temperature. Small arc-melted ingots of the composites were heat treated to investigate the stability of the eutectic microstructures. Initially, the as-cast microstructures for each eutectic was extremely fine. However, even after heat treating near the melting temperature (1625–1725 K for up to 4 h), the spacings between phases was still relatively small, (Fig. 2). Furthermore, all the eutectic phases were still present and no evidence of a solid state phase transformation was found. Hence, the phases of the eutectic microstructures were stable for the temperature range examined.

Ni–Al–Ta–Mo system

Alloys examined in the NiAl–Ta–Mo system are plotted on the composition triangle shown in Fig. 3. The large undercooling provided by the water cooled hearth during arc-melting produced microstructures that were difficult to characterize. Over a wide composition range, the material that solidified

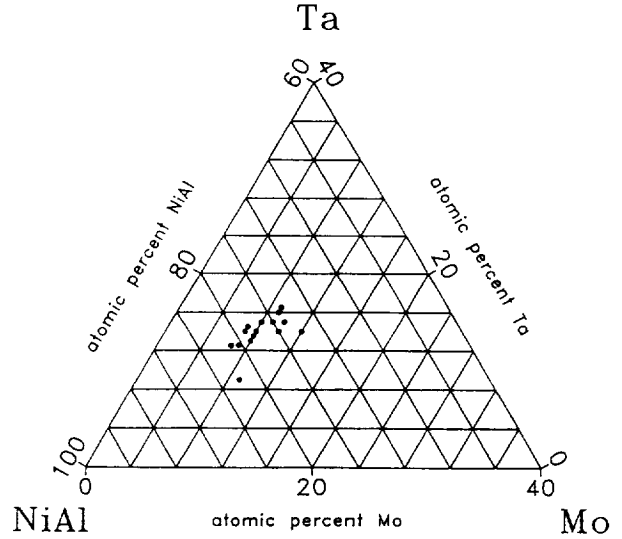

Fig. 3. Compositions of arc-melted ingots made in the NiAl–Mo–Ta system.

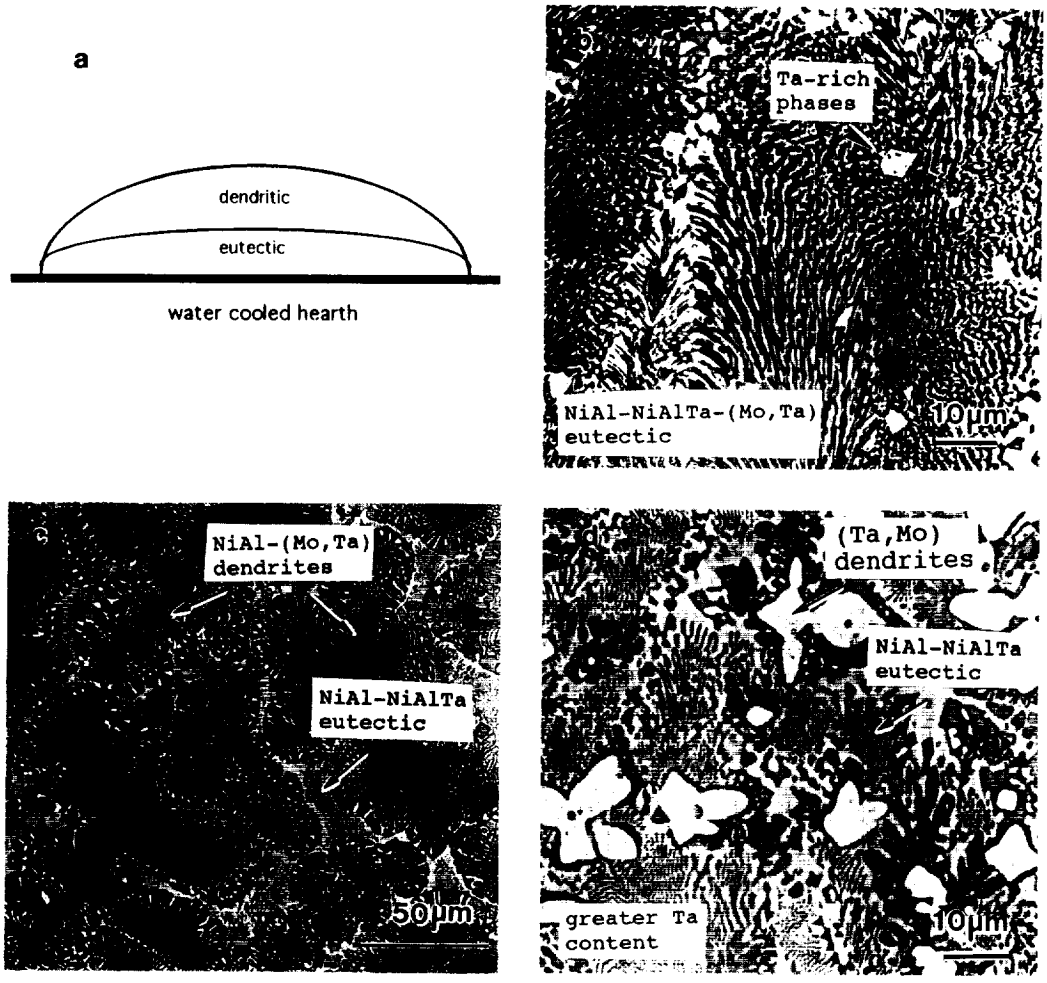

Fig. 4. Different microstructures between the bottom and the top of an arc-melted ingot in the NiAl–Mo–Ta system.

adjacent to the water cooled hearth consisted of an eutectic-like microstructure whereas the rest of the ingot was dendritic in nature (Fig. 4). The morphology of the dendritic region was dependent upon the orginal composition of the ingot. The compositions in Fig. 3 with the greater precentages of NiAl resulted in two-phase dendrites consisting of NiAl + Mo, Fig. 4(c). Conversely, greater percentages of Ta resulted in (Ta, Mo) dendrites, Fig. 4(d). A composition of Ni–42Al–12·5Ta–7·0Mo (at.%) resulted in the largest volume fraction of eutectic material in either the arc-melted or induction melted ingots. However, the nominal melting temperature (1800 K) of this alloy was greater than that of the NiAl–Mo eutectic (1778 K),[10] indicating an off-eutectic composition. Ingots of the above composition were directionally solidified at 19 mm/h for mechanical property testing.

The longitudinal microstructure from a directionally solidified ingot is shown in Fig. 5. The NiAl–NiAlTa–(Mo, Ta) ternary eutectic consists of a lamellar microstructure between NiAl and NiAlTa. A fibrous morphology is found for the molybdenum-rich solid solution that is surrounded completely by NiAl. The directionally solidified microstructure consisted of some regions of well-aligned three phase material while other areas contained NiAl + (Mo, Ta) two phase dendrites and the two phase NiAl–NiAlTa eutectic microstructure similar to the microstructure in Fig. 4(c).

The phase compositions were determined for an arc-melted ingot heat treated at 1673 K for 14·4 ks (4 h). These results, along with a schematic of the projected liquidus troughs are shown in Fig 6. The relative amounts of each phase determined by lever rule calculations from Fig. 6 compare reasonably well with the area fractions' measurements listed in Table 1.

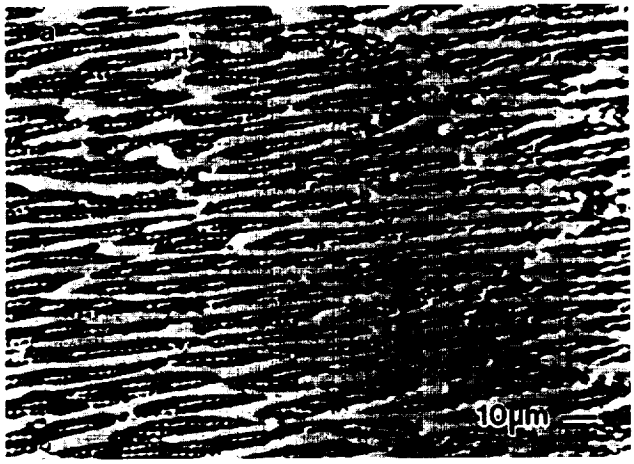

Fig. 5. Longitudinal SEM photomicrographs of the directionally solidified NiAl–NiAlTa–(Mo, Ta) eutectic.

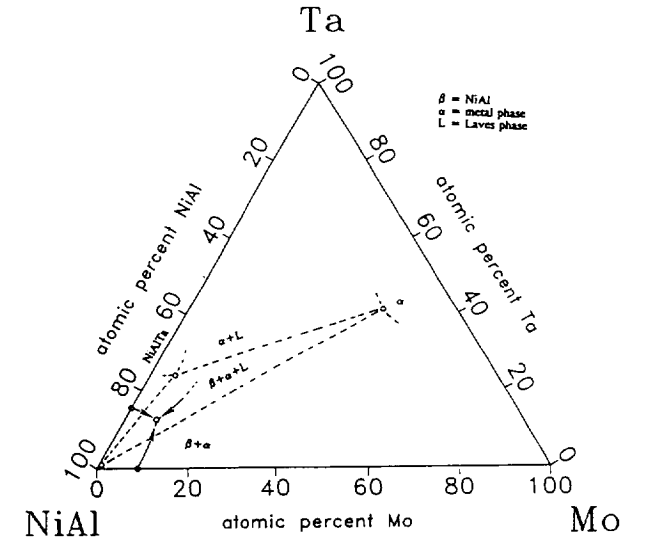

Fig. 6. Compositions of the eutectic phases at 1673 K and a schematic of the projected liquidus troughs in the NiAl–Mo–Ta system.

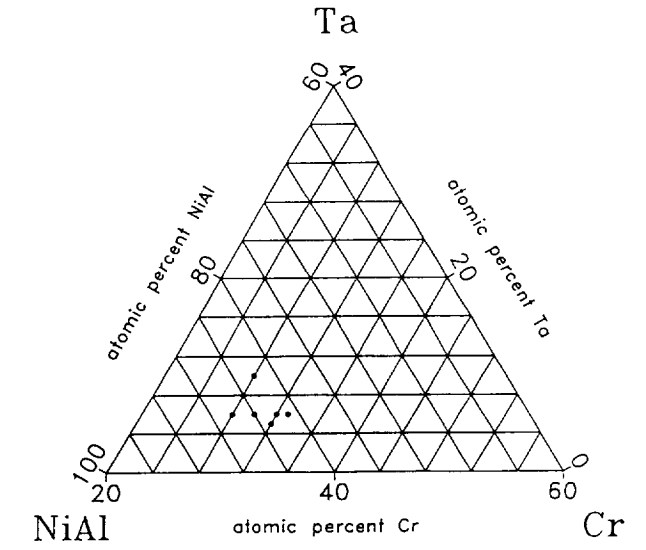

Fig. 7. Compositions of arc-melted ingots made in the NiAl–Cr–Ta system.

Ni–Al–Ta–Cr system

Alloys examined in the Ni–Al–Ta–Cr systems are plotted in the composition triangle shown in Fig. 7. Arc-melted ingots in this system were much easier to produce than the Ni–Al–Ta–Mo systems since no abrupt changes in microstructure were observed. From the survey study, an ingot with a composition of Ni–33Al–28Cr–6Ta (at.%) was cast and directionally solidified at 19 mm/h for further study.

The phase compositions were determined for an arc-melted ingot heat treated at 1673 K for 14·4 ks (4 ha). These results, along with a schematic of the projected liquidus troughs are shown in Fig. 8. As indicated in Fig. 8, a possible continuous solid solution between the NiAlTa and the Cr_2Ta Laves phases exists.

The longitudinal microstructure from the directionally solidified ingot is shown in Fig. 9. The microstructure of this ingot was essentially all eutectic. The NiAl–(Cr, Al) NiTa–Cr ternary eutectic consists of an NiAl matrix containing chromium rods and laths of the Laves phase. The relative amounts of each phase determined by the lever rule differed from those determined from the area fractions, (Table 1). The difference in these values are probably due to errors in measuring the area fractions. The atomic number contrast of the NiAl and chromium phases were similar making an accurate determination from the SEM backscattered electron image difficult. The morphology of this eutectic is more clearly shown in Fig. 10. The greater resolution of the TEM image clearly shows the fine structure.

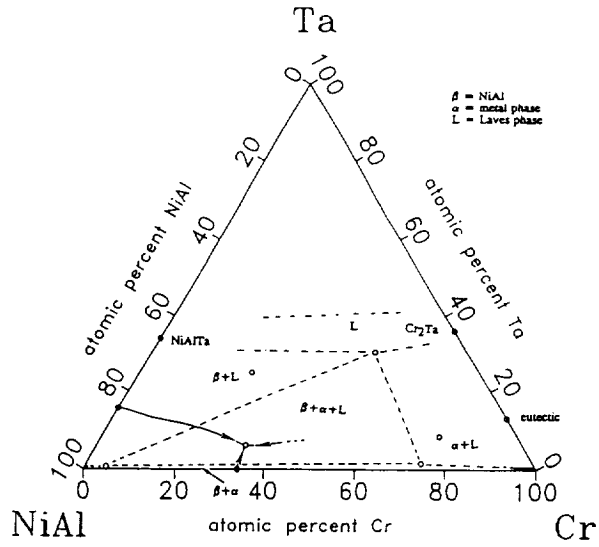

Fig. 8. Compositions of the eutectic phases at 1673 K and a schematic of the projected liquidus troughs in the NiAl–Cr–Ta system.

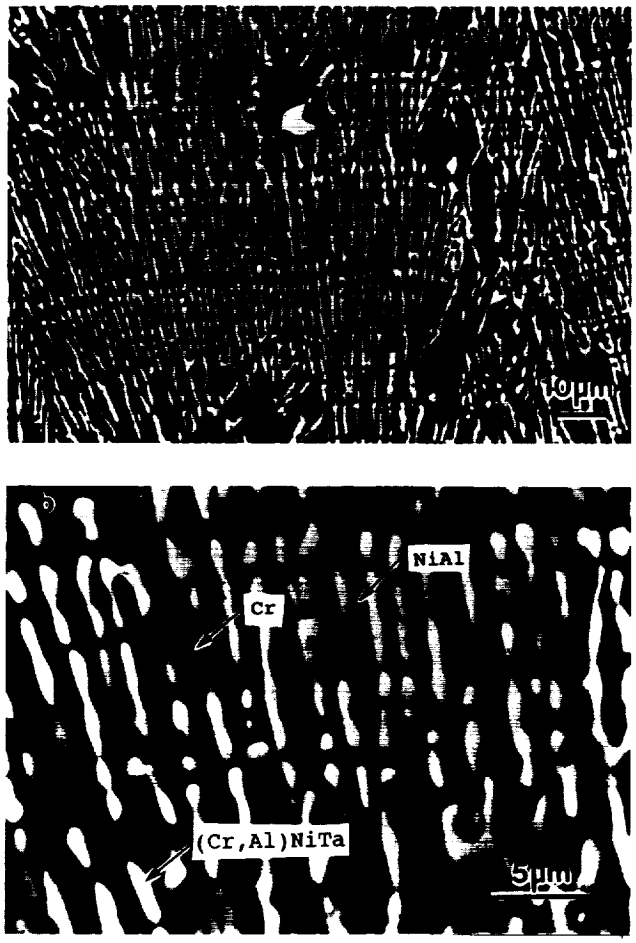

Fig. 9. Longitudinal SEM photomicrographs of the directionally solidified NiAl–(Cr, Al)NiTa–Cr eutectic.

Fig. 10. TEM photomicrograph of an arc-melted NiAl–(Cr, Al)NiTa–Cr eutectic.

Ni–Al–Ta–V system

Compositions studied in the Ni–Al–Ta–V systems are shown in Fig. 11. Based on the survey study, a near eutectic composition of Ni–28·5Al–10Ta–33V was directionally solidified at 19 mm/h for further

study. The microstructure of the directionally solidified ingot consisted of vanadium-rich dendrites surrounded by cells or colonies of the three phase eutectic. The eutectic cells were not aligned along the growth axis of the ingot. The eutectic microstructure is shown in Fig. 12. This eutectic is different than the previous two in that the Laves phase contacts both the NiAl and the metal phase. The eutectic microstructure is characterized by a lamellar morphology between NiAl and vanadium-rich metal phase with the Laves phase having a faceted rod type morphology. Figure 12 consists of microstructures taken from two different sections of the same directionally solidified ingot and is characteristic of the poor alignment of this material.

The phase compositions determined from an arc-melted ingot heat treated at 1533 K for 14·4 ks (4 h) are shown in Fig. 13 along with a schematic of the projected liquidus troughs. The relative amounts of each phase as determined by the lever rule calculations and area fractions measurements are in good agreement (Table 1).

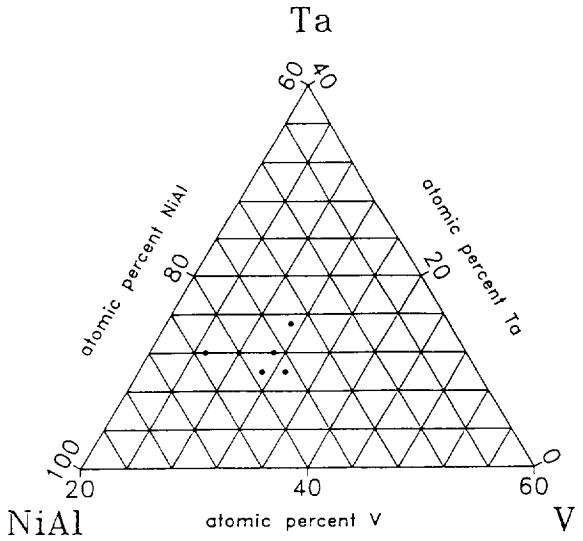

Fig. 11. Compositions of arc-melted ingots made in the NiAl–V–Ta system.

Fig. 12. Longitudinal SEM photomicrographs of the directionally solidified NiAl–NiAlTa–V eutectic.

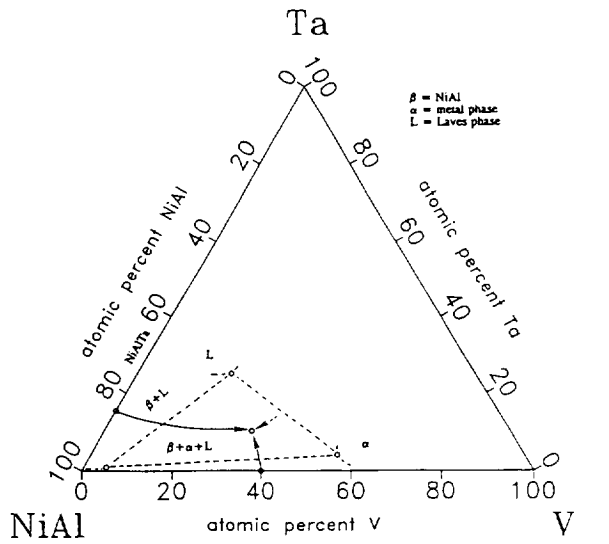

Fig. 13. Compositions of the eutectic phases at 1533 K and a schematic of the projected liquidus troughs in the NiAl–V–Ta system.

Table 2. Representative creep behavior of NiAl–(Cr, Al)NiTa–Cr and NiAl–NiAlTa–(Mo, Ta) eutectic alloys

Alloy	Representative creep behavior
NiAl–(Cr, Al)NiTa–Cr	1100–1300 K
	High stress exponent regime $\varepsilon = (9{\cdot}43 \times 10^{-13})\sigma^{10{\cdot}29}\exp(-422{\cdot}2/RT)$
	Low stress exponent regime $\varepsilon = (7{\cdot}84)\,\sigma^{5{\cdot}22}\exp(-445{\cdot}2/RT)$
NiAl–NiAlTa–(Mo, Ta)	1200 K $\varepsilon = (2{\cdot}13 \times 10^{-22})\sigma^{6{\cdot}18}$
	1300-1400 K $\varepsilon = (7{\cdot}73 \times 10^{-2})\sigma^{3{\cdot}6}\exp(-317{\cdot}9/RT)$

ELEVATED TEMPERATURE STRENGTH

Compressive creep strength of the NiAl–Ta–Mo and the NiAl–Ta–Cr alloys was determind within the temperature range of 1100–1400 K. The flow stress, σ, and strain rate, ε, data for these alloys were fitted to a temperature compensated-power law equation:

$$\varepsilon = A\sigma^n \exp(-Q/RT)$$

where A is a constant, σ is the steady state creep strength (MPa), Q is the activation energy for deformation (kJ/mol), T is the absolute temperature, R is the gas constant, and n is the stress exponent. The compressive creep characteristics for the ternary eutectics are listed in Table 2 and the corresponding data over the temperature range of 1100–1400 K are plotted in Figs 14 and 15.

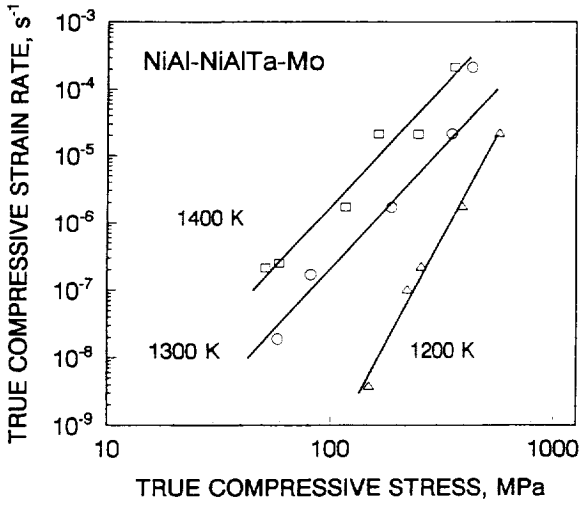

Fig. 14. Compressive flow stress–strain rate behavior for the NiAl–NiAlTa–(Mo, Ta) eutectic as a function of temperature.

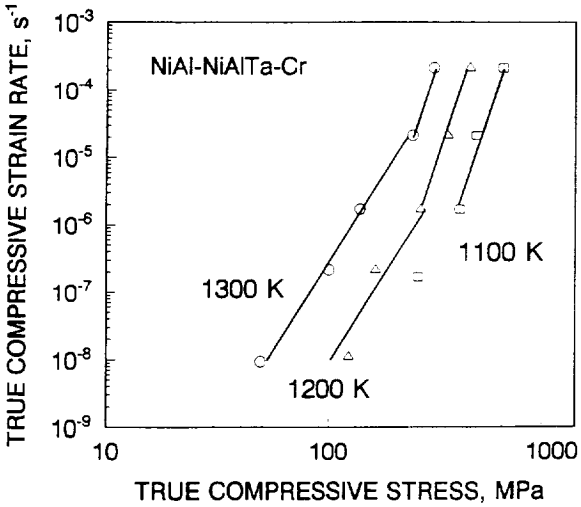

Fig. 15. Compressive flow stres–strain rate behavior for the NiAl–(Cr, Al)NiTa–Cr eutectic as a function of temperature.

For the NiAl–(Cr, Al)NiTa–Cr eutectic, there may be two creep regimes characterized by similar activation energies but having different stress exponents. A similar result is found for the NiAl–NiAlTa–(Mo, Ta) eutectic where a different equation is needed to describe the 1200 K creep behavior. The lower stress exponent at low deformation rates are likely to be due to a decrease in the ductile to brittle transition temperature (DBTT) of the ternary eutectic alloys, compared to the NiAl–NiAlTa binary system. Sauthoff has shown that DBTT is a function of deformation rates in the NiAl–NiAlTa alloys and decreases with smaller percentages of the Laves phase.[11] The volume fraction of Laves phase in both ternary eutectics is less than that of the NiAl–NiAlTa eutectic (Table 1).

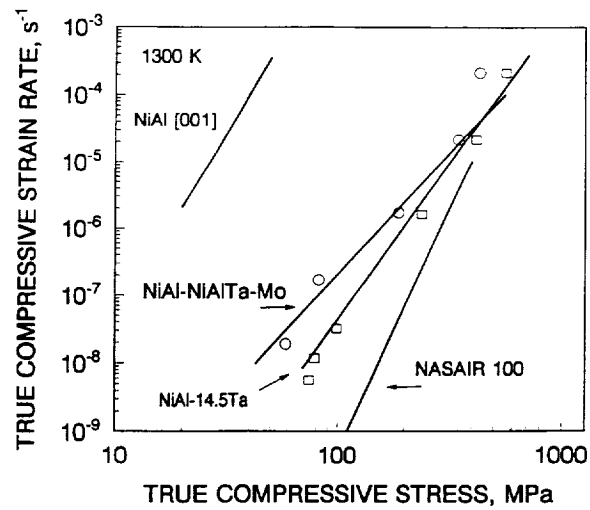

Fig. 16. 1300 K compressive flow stress–strain rate behavior for the NiAl–NiAlTa–(Mo, Ta) ternary eutectic compared to NiAl and the NiAl–NiAlTa eutectic.

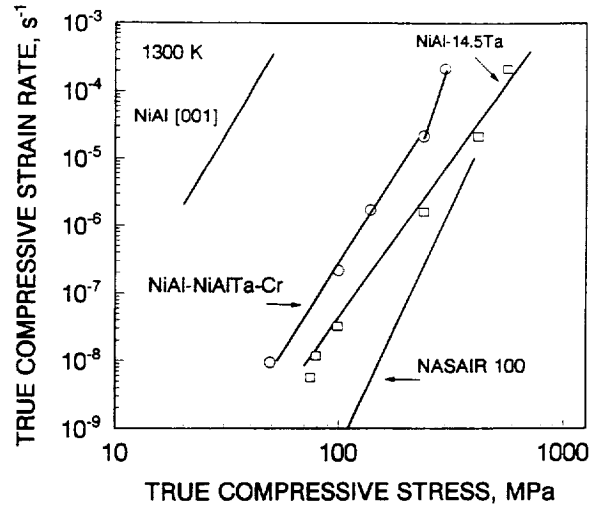

Fig. 17. 1300 K compressive flow stress–strain rate behavior for the NiAl–(Cr, Al)NiTa–Cr ternary eutectic compared to NiAl and the NiAl–NiAlTa eutectic.

In Figs 16 and 17, the 1300 K compressive strength of both the NiAl–NiAlTa–(Mo, Ta) and the NiAl—(Cr, Al)NiTa–Cr eutectics are compared to single crystal NiAl and the NiAl–NiAlTa eutectic. The 1300 K creep strength of both ternary eutectics are substantially greater than that of binary NiAl but are less than that of the NiAl–NiAlTa eutectic.

ROOM TEMPERATURE TOUGHNESS

The room temperature fracture toughness values for the NiAl–NiAlTa–refractory metal eutectics are listed in Table 3. The fracture toughness of the NiAl–(Cr, Al)NiTa–Cr eutectic (15 MPa$\sqrt{m}$) lies between that of the NiAl–NiAlTa eutectic (5 MPa$\sqrt{m}$) and that of the NiAl–Cr eutectic (20 MPa$\sqrt{m}$). However the fracture toughness for the NiAl–NiAlTa–(Mo, Ta) and NiAl–NiAlTa–V eutectics were only slightly greater than that of the NiAl–NiAlTa eutectic.

Since the composition of the directionally solidified NiAl–Ta–Mo ingot was off eutectic, a number of heat treatments were performed in an attempt to increase the volume fraction of the metal phase. It was hoped that by heat treating in the three phase region below the ternary eutectic temperature, a more homogenous distribution of the metal phase might result. However, a coarsening of the metal phase resulted and no significant improvement in the fracture toughness was measured. The fracture surface from the NiAl–Ta–Mo bend sample is shown in Fig. 18. By comparing secondary and backscattered electron images of the fracture surface, the brittle behavior of this alloy is clearly due to the large volume fraction of the Laves phase. The fracture surface is characterized by cleavage of the Laves phase.

Table 3. Room temperature fracture toughness of NiAl–NiAlTa–refractory metal eutectics

Alloy	Fracture Toughness MPa$\sqrt{m}$
NiAl–NiAlTa–(Mo, Ta) as-processed	5·2
(Ni–42Al–12·5Ta–7Mo)	5·2
Heat treated 1625 K, 3600 s (1 h)	6·4
	6·8
Heat treated 1725 K, 9000 s (2·5 h)	6·7
	9·1
Heat treated 1725 K, 14.4 × 10^3 s (4 h)	5·7
	5·7
NiAl–(Cr, Al)NiTa–Cr as-processed	15·1
(Ni–30.5Al–6Ta–33Cr)	15·9
	15·2
	13·6
NiAl–NiAlTa–V as-processed	8·2
Ni–28.5Al–10Ta–33V)	8·7
	8·5
	7·9

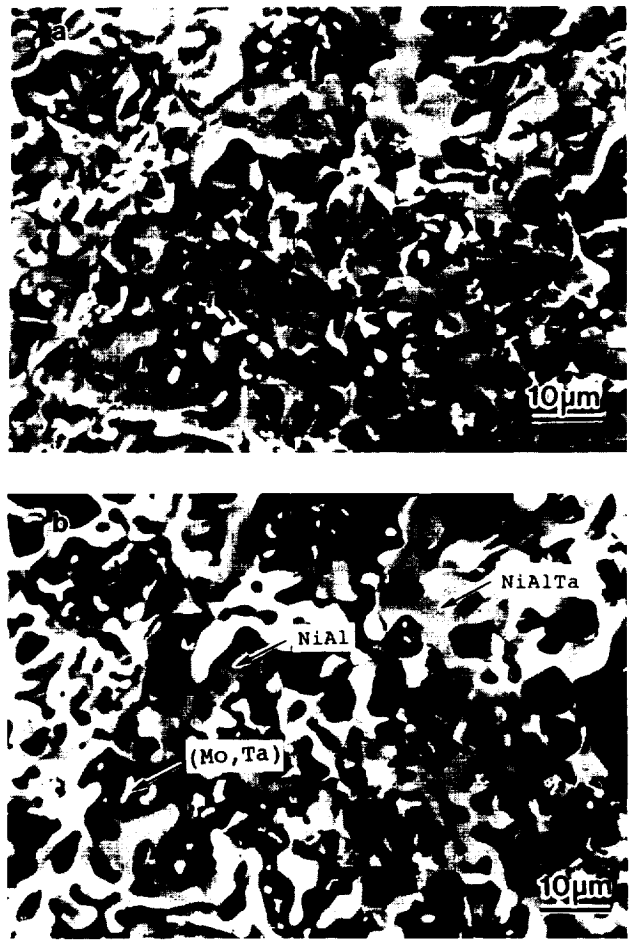

Fig. 18. SEM photomicrographs of the fracture surface of a broken NiAl–NiAlTa–(Mo, Ta) bend specimen. (a) Secondary electron image, and (b) backscattered electron image.

Conversely, the NiAl–Ta–Cr eutectic contains a smaller percentage of the Laves phase and hence has a greater fracture toughness. The fracture surface for this alloy is shown in Fig. 19. The mode of fracture is the phase boundary fracture between the NiAl phase and the Laves phase. In addition, cleavage of the NiAl phase is also observed.

Lastly, the fracture surface for the NiAl–NiAlTa–V eutectic is shown in Fig. 20. The fracture surface for this alloy closely resembles the eutectic microstructure. The toughness of this material was poor. This is attributed to the result that almost no alignment of the phases was produced on directional solidification. The poor alignment is due to the formation of a cellular microstructure upon directional solidification.

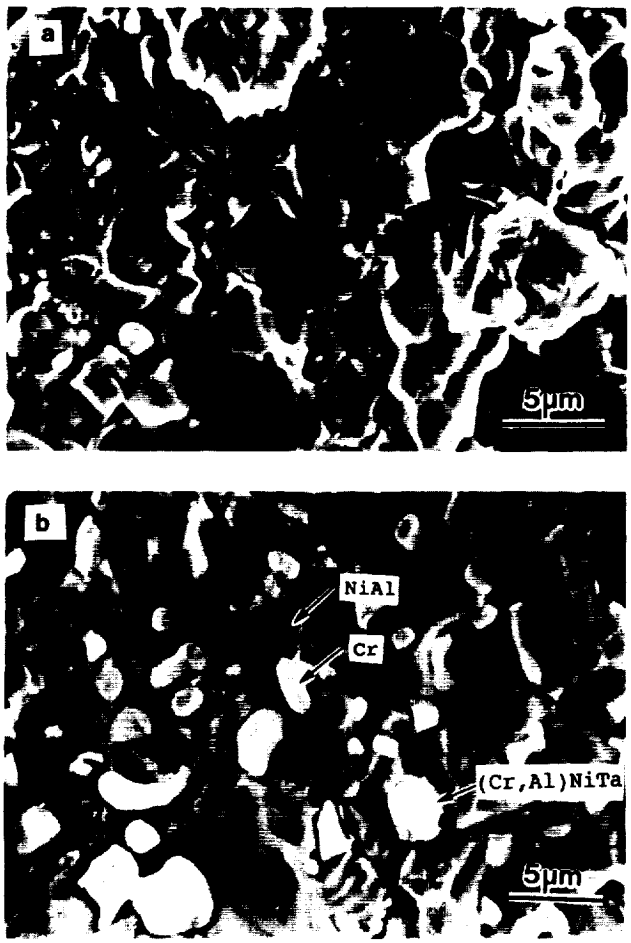

Fig. 19. SEM photomicrographs of the fracture surface of a broken NiAl–(Cr, Al)NiTa–Cr bend specimen. (a) and (b) secondary electron image, and (c) backscattered electron image.

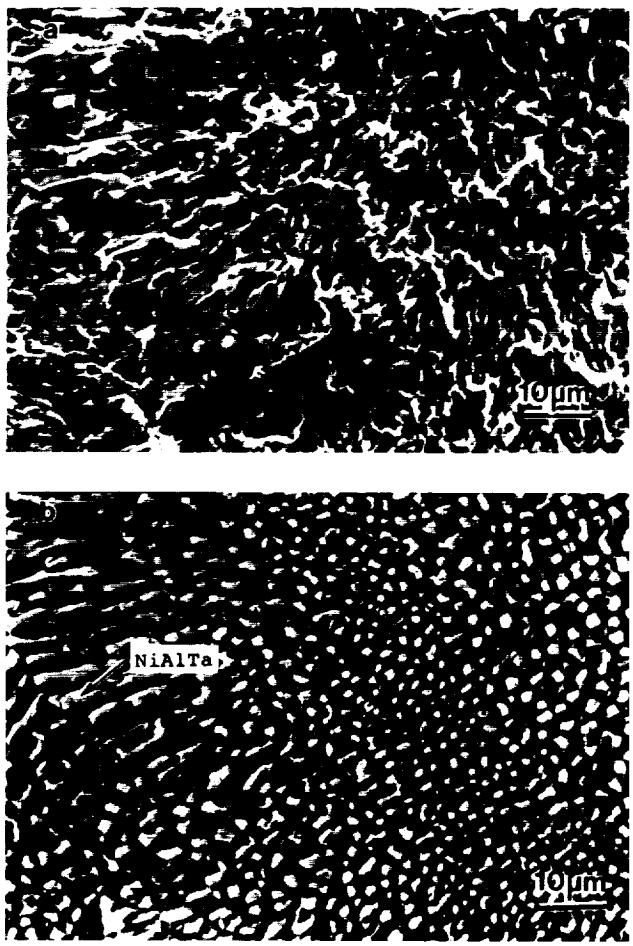

Fig. 20. SEM photomicrographs of the fracture surface of a broken NiAl–NiAlTa–V bend specimen. (a) Secondary electron image, and (b) backscattered electron image.

DISCUSSION

The performance of the eutectic alloys in terms of the room temperature fracture toughness and the compressive creep strength varied greatly depending upon the volume fraction and morphology of the eutectic phases. For example, the Nial–NiAlTa–(Mo, Ta) eutectic contained a large volume fraction of the brittle Laves phases in the form of a continuous lamellar layer. Hence, this alloy was very brittle. Conversely, the large volume fraction of a ductile metallic phase in NiAl–NiAlTa–V eutectic provided no improvement in the fracture toughness. The poor alignment of the microstructure allowed crack propagation to follow the more brittle intermetallic phases. However, there was an improvement in the fracture toughness of the NiAl(Cr, Al)NiTa–Cr when compared to that of the NiAl–NiAlTa eutectic. The Laves phase in the ternary eutectic was in the form of discontinuous rods. It is interesting to note that the fracture mode of the NiAl–(Cr, Mo)NiTa–Cr eutectic was by interphase fracture and not by cleavage as was found in the binary NiAl–Cr and NiAl–NiAlTa eutectics.[1,2] Thus, one possibility for further improving the fracture toughness of the ternary eutectic would be by locating an interstitial alloy addition that would improve the phase boundary strength without lowering the stress needed to initiate cleavage fracture.

In terms of the high temperature strength, the lower melting temperature of the ternary eutectics should result in a decrease in strength when compared to the individual binary eutectics. In Fig. 21 the 1300 K creep strength for the directionally solidified binary and ternary eutectics are plotted against the corresponding room temperature fracture toughness. The creep strength of the ternary eutectics was always less than that of the NiAl–NiAlTa eutectic due to the decrease in the volume fraction of the Laves phase and the lower melting temperature. However, for both the NiAl–NiAlTa–

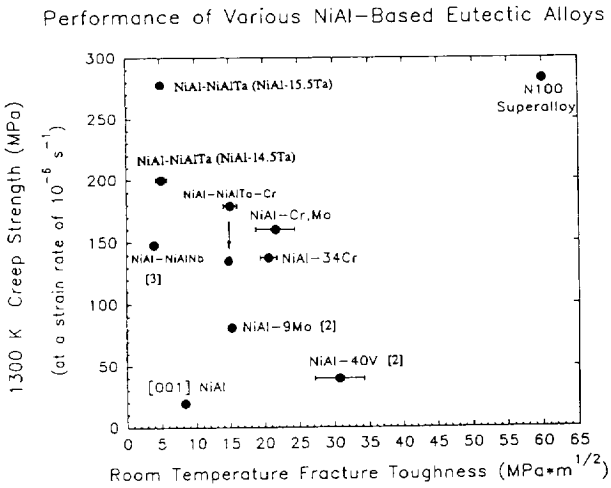

Fig. 21. Performance of NiAl-based directionally solidified eutectics compared to binary single crystal NiAl and a single crystal superalloy.

(Mo, Ta) and the NiAl–(Cr, Al)NiTa–Cr eutectics, the creep strength of the ternary eutectic was greater than that of the simple NiAl–refractory metal eutectics.

As described previously, two equations are needed to characterize the deformation behavior for the NiAl–(Cr, Al)NiTa–Cr eutectic over the strain rates and temperatures examined. At high strain rates ($> 10^{-5}$ s^{-1}, 1300 K) the strength of the ternary eutectic was intermediate between those of the NiAl–NiAlTa and the NiAl–Cr eutectics. However, at lower strain rates, the creep strength of the ternary eutectic decreased to values near those of the NiAl–Cr eutectic. The change in the creep behavior for the NiAl–(Cr, Al)NiTa–Cr eutectic is shown in Fig. 21 where calculated values of both the high stress exponent and the low stress exponent behavior are given. Conversely, deformation of all of the binary eutectics could be described with one equation under similar conditions.[1,2] Hence, one reason for the change in the creep behavior of the ternary eutectic at the lower deformation rates may be due to the addition of another phase boundary. Simply, the increased interfacial area may increase the number of nucleation sites for thermally generated defects.

Finally, the goal of this research was to discover if a balance of properties could be achieved by combining the properties of the individual binary eutectics in a multiphase alloy. Of the alloys studied, the ternary eutectic in NiAl–Ta–Cr system came the closest to achieving this goal. In addition, since NiAl, NiAlTa, and Cr are all thermodynamically compatible, conventional techniques to produce composite materials formed by joining materials containing the NiAl–NiAlTa and the NiAl–Cr eutectics may also be possible. The ternary eutectic represents the lowest melting temperature (1700 K) for alloy compositions within the NiAl, Laves phase, and chromium three phase region as shown in Fig. 8. However, the melting point of the ternary eutectic at 1700 K is not significantly lower than that of the NiAl–Cr binary eutectic (1718 K).[10] From the preliminary mechanical priority data, the creep resistance of the ternary eutectic is similar to that of the NiAl–Cr eutectic and the fracture toughness is greater than that of the NiAl–NiAlTa eutectic.

CONCLUSIONS

Ternary eutectics consisting of NiAl, a Laves phase, and a metallic phase were located in the NiAl–Ta–*X* (*X* = Cr, Mo, and V) systems. Directional solidification of the Cr and Mo containing eutectics produced polyphase *in situ* composites where the phases were aligned parallel to the growth direction. The NiAl–(Cr, Al)NiTa–Cr eutectic displayed the best combination of room temperature fracture toughness and the elevated temperature strength and was intermediate between the properties of the separate NiAl–NiAlTa and NiAl–Cr eutectics.

REFERENCES

1. Johnson, D. R., Chen, X. F., Oliver, B. F., Noebe, R. D. & Whittenberger, J. D., Processing and mechanical properties of *in situ* composites from the NiAl–Cr and NiAl–(Cr, Mo) eutectic system, *Intermetallics*, **3** (1995) 99–113.
2. Johnson, D. R., Chen, X. F., Oliver, B. F., Noebe, R. D. & Whittenberger, J. D., Directional solidification and mechanical properties of NiAl–NiAlTa alloys, *Intermetallics*, **3** (1995) 141–52.
3. Noebe, R. D., Bowman, R. R. & Nathal, M. V., *Int. Mat. Rev.*, **38** (1993) 193–232.
4. Joslin, Steve, Ph.D. thesis, University of Tennessee (in progress).
5. Durand-Charre, M., David, D. & Wang, J., *High Temp. Mat. and Proc.*, **10** (1991) 1–12.
6. Chakravorty, S. & West, D. R. F., *Mat Sci. and Tech.*, **1** (1985) 978–85.
7. Chakravorty, S. & West, D. R. F., *Metal Sci.*, **18** (1984) 207–15.
8. Chakravorty, S., Sadiq, S. & West, D. R. F., *J. Mat. Sci.*, **24** (1989) 577–83.
9. Johnson, D. R., Joslin, S. M., Reviere, R. D., Oliver, B. F. & Noebe, R. D., In *Processing and Fabrication of Advanced Materials for High Temperature Applications–II*, eds V. A. Ravi & T. S. Srivatsan, TMS, Warrendale, PA, 1993, pp. 77–90.
10. Cline, H. E., Walter, J. L., Lifshin, E. & Russel, R. R., *Met. Trans.*, **2** (1971) 189.
11. Sauthoff, G., In *Structural Intermetallics*, eds R. Darolia *et al.*, TMS, Warrendale, PA, 1993, pp. 371–8.